Applied Geochemistry 27 (2012) 211–222

Contents lists available at SciVerse ScienceDirect

Applied Geochemistry

journal homepage: www.elsevier.com/locate/apgeochem

Spatial–temporal variations of travertine deposition rates and their controlling factors in Huanglong Ravine, China – A world's heritage site

Jinliu Zhang [a], Haijing Wang [a], Zaihua Liu [a,*], Dejun An [b], Wolfgang Dreybrodt [c]

[a] The State Key Laboratory of Environmental Geochemistry, Institute of Geochemistry, Chinese Academy of Sciences, Guiyang 550002, China
[b] Huanglong National Scenic Spot Administration, Songpan 623300, China
[c] Karst Processes Research Group, University of Bremen, Bremen 28359, Germany

ARTICLE INFO

Article history:
Received 6 May 2011
Accepted 20 October 2011
Available online 31 October 2011
Editorial handling by I. Cartwright

ABSTRACT

Huanglong, well known for its unique natural travertine landscape, was listed by UNESCO as an entry in the World's Nature Heritage in 1992, and attracts more than one million of tourists from all over the world each year. However, the landscape has undergone significant degradation (notably, serious decay of travertine) during the past two decades as the tourist numbers have increased remarkably. To understand the variations of travertine deposition rates and their controlling factors, especially the impact of tourism activities, paired water and modern travertine samples deposited on plexiglass substrates were taken along the Huanglong stream at regular intervals from early May to early November in 2010 (i.e., in the wet season). The travertine deposition rates have declined significantly compared to those in early 90s in all four subsystems in the Huanglong Ravine. The largest decrease (89.5%) occurred at the lowest sampling site. The reduction in travertine deposition most likely resulted from the phosphate pollution caused by the tourism activities. In spite of an increase in concentrations of Ca, calcite saturation, and water temperature, which facilitate calcite precipitation, deposition rates decreased because of inhibition by PO_4^{3-} ions. Seasonally, three control patterns of travertine deposition rates were distinguished along the Ravine. They are control by water-temperature, control by dilution of rainwater and snow-melting water and control by PO_4-inhibition of calcite precipitation.

1. Introduction

Huanglong, well known for its unusual and diversified landscapes (e.g., travertine pools, travertine falls and travertine shoals, Lu and Li, 1992; Lu et al., 2000), was listed by UNESCO in 1992 as an entry in the World's Nature Heritage. Since then, tourist numbers have increased from about one hundred thousand in early 1990s to over a million in recent years. However, the Huanglong travertine landscape has also undergone significant degradation in recent years, notably the serious chemical weathering and physical decay of travertine (Liu et al., 2009). It is known that PO_4^{3-} introduced into the water by agricultural activities can inhibit deposition of travertine. This has been observed at the waterfall of Urach, Germany (Michaelis et al., 1984). Laboratory experiments (Lin and Singer, 2006) have shown that concentrations of total PO_4^{3-} above 1 μmol/L strongly inhibit precipitation of calcite at pH = 7.95. This gives rise to the suspicion that tourist activities could endanger Huanglong due to declining travertine deposition.

In order to determine whether the present day travertine deposition rates have changed compared to those in early 1990s (Liu et al., 1995), and to investigate whether increased tourist activities impact travertine deposition due to PO_4^{3-} inhibition of calcite precipitation (Reddy and Nancollas, 1973; Ralph et al., 1996; Bono et al., 2001; Plant and House, 2002), paired water samples and modern travertine calcite deposited on plexiglas substrates were collected along the Huanglong stream at regular intervals from early May to early November in 2010 (which is the wet season when travertine normally precipitates). Moreover PO_4^{3-} concentrations were measured. This information not only answers questions relevant to Huanglong but also provides a scientific basis for the protection of many travertine landscapes worldwide.

2. General setting of the study area

Huanglong is located about 360 km NW of the provincial capital, Chengdu, Sichuan Province, China on the southern slope of the Minshan Mountains that separate the Qinhai Highlands from the Sichuan Basin (Fig. 1). Because of the yellow color of the travertine and its morphological resemblance to the shape of a dragon, the location is named Huanglong (yellow dragon). Its elevation ranges from 3100 to 3600 m above sea level (asl). The geology consists of Paleozoic carbonate rocks exceeding 4000 m in thickness, overlain by about 1000 m of Mesozoic clastic rocks plus Cenozoic

* Corresponding author. Tel./fax: +86 851 5892338.
E-mail address: liuzaihua@vip.gyig.ac.cn (Z. Liu).

0883-2927/$ - see front matter © 2011 Elsevier Ltd. All rights reserved.
doi:10.1016/j.apgeochem.2011.10.005

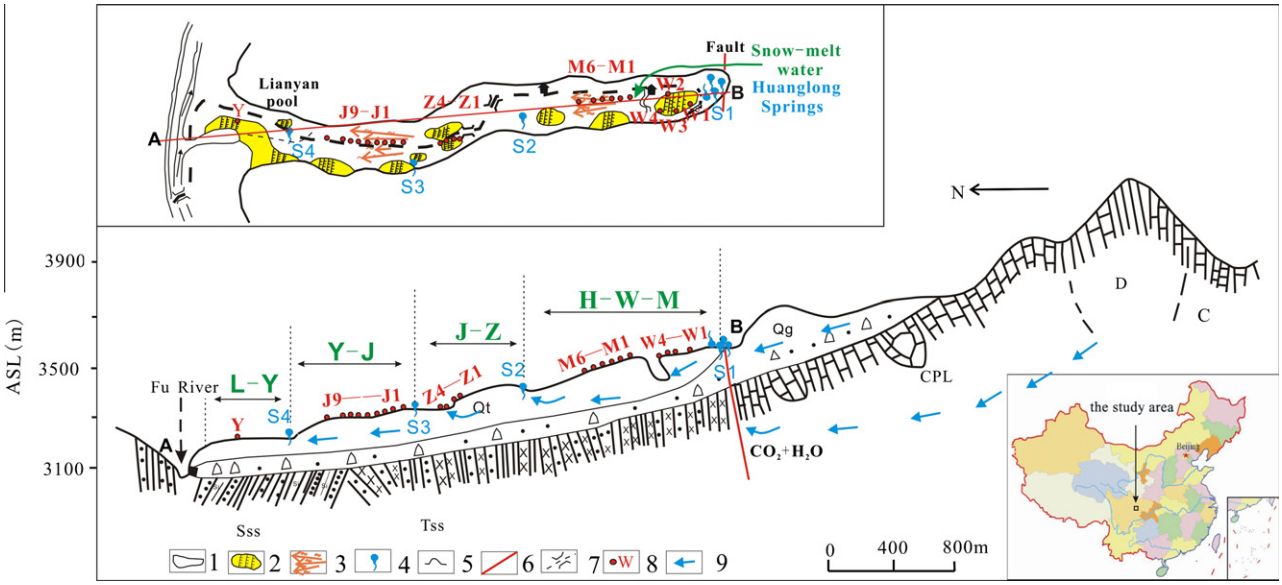

Fig. 1. Plan (top) and geological section (bottom) of Huanglong Ravine with springs and sampling sites. 1. Boundary of the travertine scenery; 2. rimstone dam and pool; 3. travertine shoal; 4. spring; 5. travertine cave; 6. fault; 7. trail; 8. sampling site; 9. flow direction of groundwater. H–W–M: Huanglong springs–Wucaichi–Matihai subsystem; J–Z: Jiexianqiao Spring–Zhengyanchi subsystem; Y–J: Yingfang Spring–Jinshapudi subsystem; L–Y: Longyan Spring–Yingbinchi subsystem. W: Wucaichi pond (four sampling sites: W1–W4); M; Matihai (six sampling sites: M1–M6); Z: Zhengyanchi (four sampling sites: Z1–Z4); J: Jinshapudi (nine sampling sites: J1–J9); Y: Yingbinchi (one sampling site). S1: Huanglong spring; S2: Jiexianqiao spring; S3: Yingfang spring; S4: Longyan spring, Qt/Qg – quaternary travertine/glacial sand and gravel; Tss – triassic sandstone and slate; CPL – carboniferous and Permian limestone; C – carboniferous limestone; D – devonian slate and limestone; Sss – silurian slate, intercalated with sandstone.

alluvial gravels, glacial moraines and travertine (Liu et al., 1995). At Huanglong, the travertine deposits have accumulated over a width of ~250 m and a length of 3.5 km (Fig. 1) in the form of travertine pools (Fig. 2), travertine falls and travertine shoals.

The average annual precipitation is 759 mm and the mean air temperature 1.1 °C (Liu et al., 1995). Groundwater discharges along a fault zone in springs (Huanglong spring group) at an altitude of about 3580 m asl, with water temperature about 5 °C higher than annual mean air temperature (Liu et al., 1995). Huanglong spring water supplies Wucaichi travertine pool (Multi-colored pools) and then mixes with glacier-snow melt water from higher mountains (the highest peak, Xuebaoding at 5588 m asl) to supply the Matihai travertine shoals (Fig. 1). Another three secondary springs, Jiexianqiao Spring, Yingfang Spring and Longyan Spring, occur further downstream along Huanglong Ravine. They supply the other three downstream scenic areas, respectively (Fig. 1).

Accordingly, downstream from each spring four subsystems in the Ravine, namely Huanglong springs–Wucaichi–Matihai subsystem (H–W–M subsystem), Jiexianqiao Spring–Zhengyanchi subsystem (J–Z subsystem), Yingfang Spring–Jinshapudi subsystem (Y–J subsystem) and Longyan Spring–Yingbinchi subsystem (L–Y subsystem) were distinguished (H–W–M, J–Z, Y–J and L–Y, respectively in Fig. 1). In the text these names are used to specify the locations.

Fig. 2. Photograph of the famous Wucaichi (multi-colored pools) landscape.

3. Methods

To understand temporal-spatial variations in modern travertine deposition rates and water chemistry in Huanglong Ravine, 24 monitoring and sampling sites in the four subsystems, were set up, defined by the geomorphic differences.

3.1. Installation and collection of plexiglass substrates and measurement of modern travertine deposition rates

In order to obtain modern travertine (carbonate) deposition rates, plexiglass collector substrates measuring 5 cm × 5 cm × 0.5 cm (with an aggregate surface area of 60 cm^2 each) were mounted in the flowing water in the monitoring sites in the four subsystems (Liu et al., 1995, 2010). The substrate has a hole of 5 mm diameter in its center and was screwed to a steel nail, which had been fixed to the travertine bed of the river. The faces of the substrates were oriented parallel to the flow and the riverbed. Some samples were located in fast flowing water, 2 cm below the water surface, whereas others were mounted 10 cm beneath the water surface in a pool with standing water. Fig. 3 shows such a substrate mounted in the pool.

The substrates were replaced every 10 days; the amount of travertine deposited on them was determined by measuring the weight increase of the plexiglass substrate. Before immersion and after collection each plexiglass substrate was dried at 50 °C for a period of 24 h and cooled to room temperature in a glass dryer and then weighed. The carbonate deposition rate (R) was calculated by:

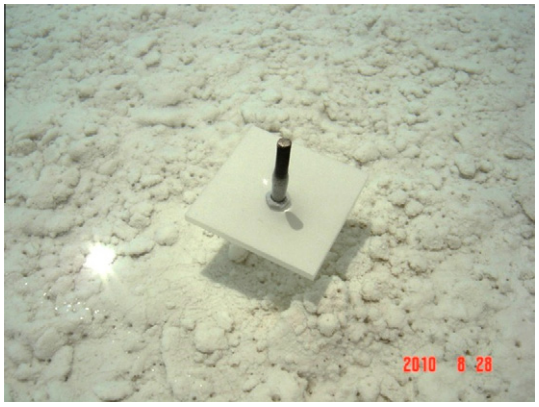

Fig. 3. Photograph at one of the experimental sites. The sample holder represents the Wucaichi pool site location with still water conditions.

$$R = \frac{(W_{ts} - W_s)}{A \times T}$$

where W_{ts} and W_s are the weight of the plexiglass substrate after and before each experimental run, respectively, A is the surface area of the substrate (60 cm^2) exposed to the water, and T is the exposure time for carbonate precipitation on the plexiglas substrate for each run (~10 days). Water evaporating during drying will not significantly contribute to the amount of calcite precipitated. The average mass of $CaCO_3$ precipitated in the 10 days is 8 mg. The river water contains approximately 0.25 g/L of $CaCO_3$. Even if a water film with a depth of 0.02 cm remained for evaporation, which is unlikely, only 0.3 mg of calcite could be precipitated from it.

The material deposited covered the substrate as a layer with a thickness of about 4 μm. Fig. 4 shows a substrate before it was immersed in the water and after 10 days exposure to travertine deposition. The material deposited on it was analyzed by XRD using CuKα radiation and found to consist of pure calcite without any traces of other phases, such as vaterite or aragonite. The XRD spectra were identical for all sampling sites.

Fig. 5 displays an SEM picture of the surface of a plexiglass sample after 10 days of immersion. Fig. 5a shows the area where calcite crystals have been deposited on the substrate surface, while Fig. 5b shows the deposited crystals with higher magnification. From these pictures it is inferred that deposition is mainly controlled by inorganic chemical processes, and microbiological activities can be excluded.

3.2. Measurement of the water chemistry

Water temperature, pH and specific conductivity at each monitoring site were measured *in situ* daily with a hand-held water quality data logger, Model WTW 350i, with resolution of 0.01 pH, 0.1 °C and 1 μS/cm, respectively (Liu et al., 2006). Electrodes were calibrated prior to use with pH (7 and 10) and conductivity (1412 μS/cm) standards. *In situ* titration was used to determine $[HCO_3^-]$ and $[Ca^{2+}]$ approximately every 10 days by the Aquamerck Alkalinity Test and Hardness Test. The resolutions are 6 mg/L and 1 mg/L, respectively (Liu et al., 2006). In pure limestone areas, as is the case in this study, specific conductivity fluctuations in travertine depositing stream can be attributed solely to Ca^{2+} and HCO_3^- changes, either by calcite deposition or dissolution (Liu et al., 2004; Krawczyk and Ford, 2006; Wang et al., 2010) or by dilution with rain water or snowmelt water. So, paired Ca^{2+} (or HCO_3^-) and conductivity values were correlated and regression was used to establish a time-series of Ca^{2+} and HCO_3^- changes. At Huanglong, these concentrations are linearly related to specific conductivity by the relationships (Wang et al., 2010):

$$[Ca^{2+}] = 0.2651SpC - 18.607, \quad r^2 = 0.9948 \tag{1}$$

$$[HCO_3^-] = 0.8017SpC - 54.827, \quad r^2 = 0.9951 \tag{2}$$

where brackets denote species concentrations in mg/L and SpC is specific conductivity in μS/cm at 25 °C.

Water samples at the sampling sites were collected by syringe with 0.45 μm Minisart® filters. This was performed at the sites of the plexiglass collectors, at the time of their replacement. The water samples were analyzed in the State Key Laboratory of

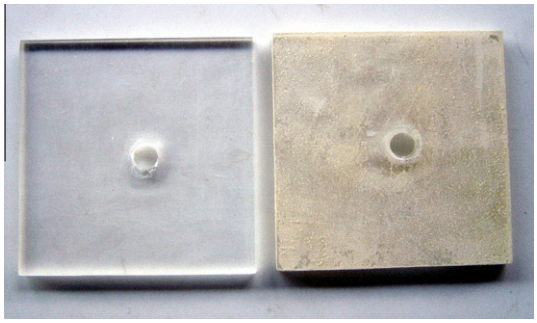

Fig. 4. Substrates before being immersed into water (left) and after 10 days exposure to travertine deposition (right).

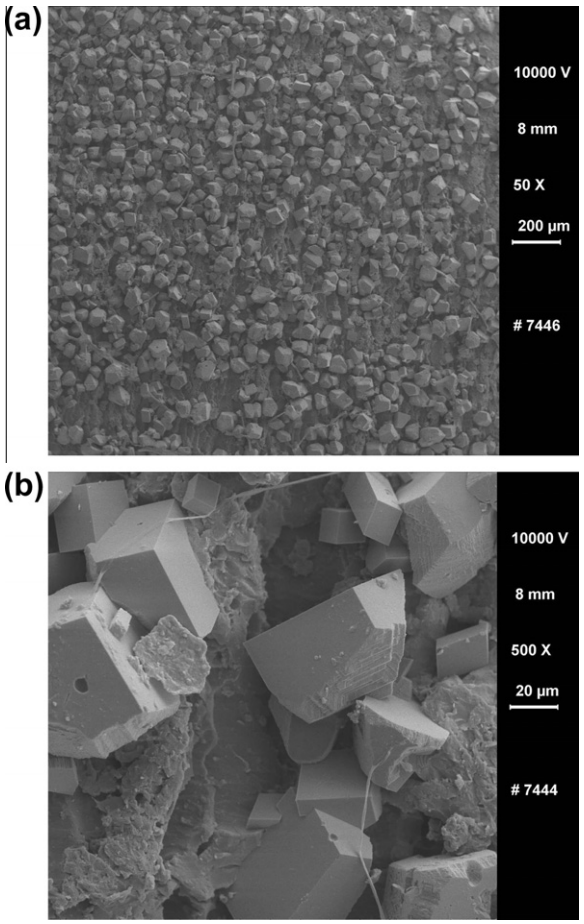

Fig. 5. Details of the structure of one of the plexiglass substrate surfaces. (a) SEM picture showing the authigenic calcite crystals deposited on the substrate surface. (b) SEM – more magnified reveals structural details of the shape and internal habit of the precipitated crystals.

Environmental Geochemistry, Institute of Geochemistry of Chinese Academy of Sciences. Concentrations of K^+, Na^+ and Mg^{2+} were determined by Inductively Coupled Plasma Optical Emission Spectrometry (Model Vista MPX) and those of Cl^-, PO_4^{3-} and SO_4^{2-} by ion chromatography (Model ICS-90) (Liu et al., 2010).

3.3. Calculation of calcite saturation index

The full hydrochemical data sets, including recorded temperature and pH, calculated Ca^{2+} and HCO_3^- through the relationships mentioned above, and the average concentrations of K^+, Na^+, Mg^{2+}, Cl^- and SO_4^{2-}, were processed with the program WATSPEC (Wigley, 1977), which calculates calcite saturation index (SIc) for each record. SIc is calculated from:

$$\mathrm{SIc} = \log\left(\frac{(Ca^{2+})\left(CO_3^{2-}\right)}{K_c}\right)$$

where activities are denoted by parentheses and K_c is the temperature dependent solubility constant for calcite. If SIc > 0, water is supersaturated with respect to calcite and may deposit it, if

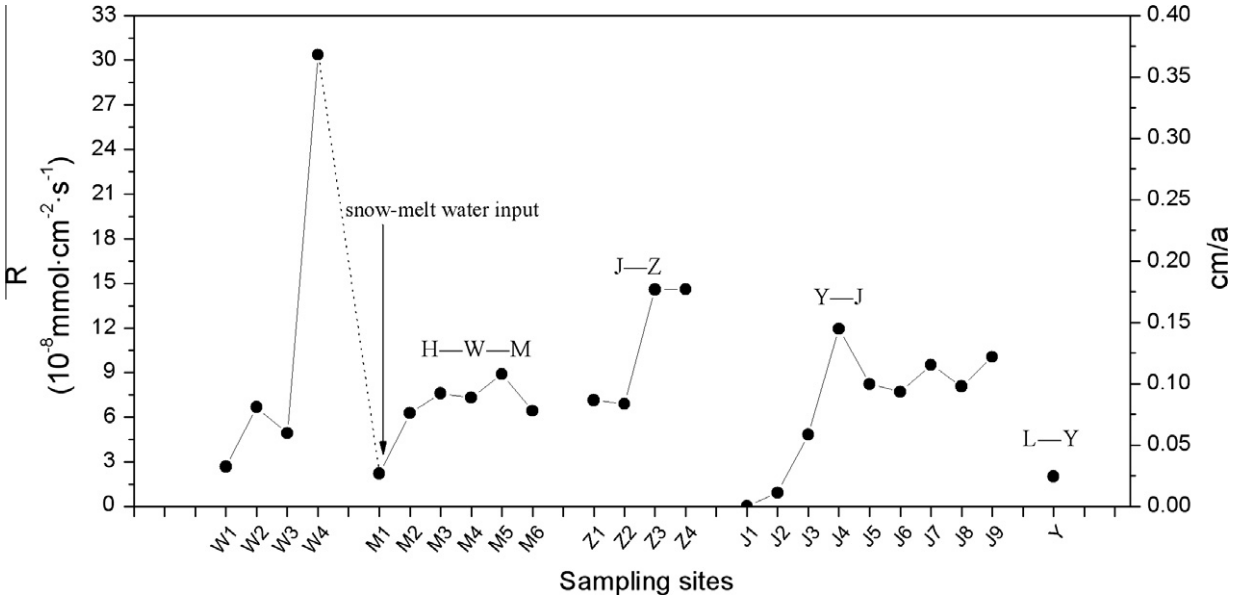

Fig. 6. Annual mean calcite deposition rate at each sampling sites in four subsystems. W1–W4 and M1–M6 belong to H–W–M subsystem; Z1–Z4: J–Z subsystem; J1–J9: Y–J subsystem; Y: L–Y subsystem. Plexiglass collector substrate at sampling site W4 was placed on rimstone dam where fast flow occurred; other plexiglass collector substrates were placed in travertine pool or streambed with slow flow. It was found that higher calcite deposition rates in each subsystem often occurred at sites with fast flowing water.

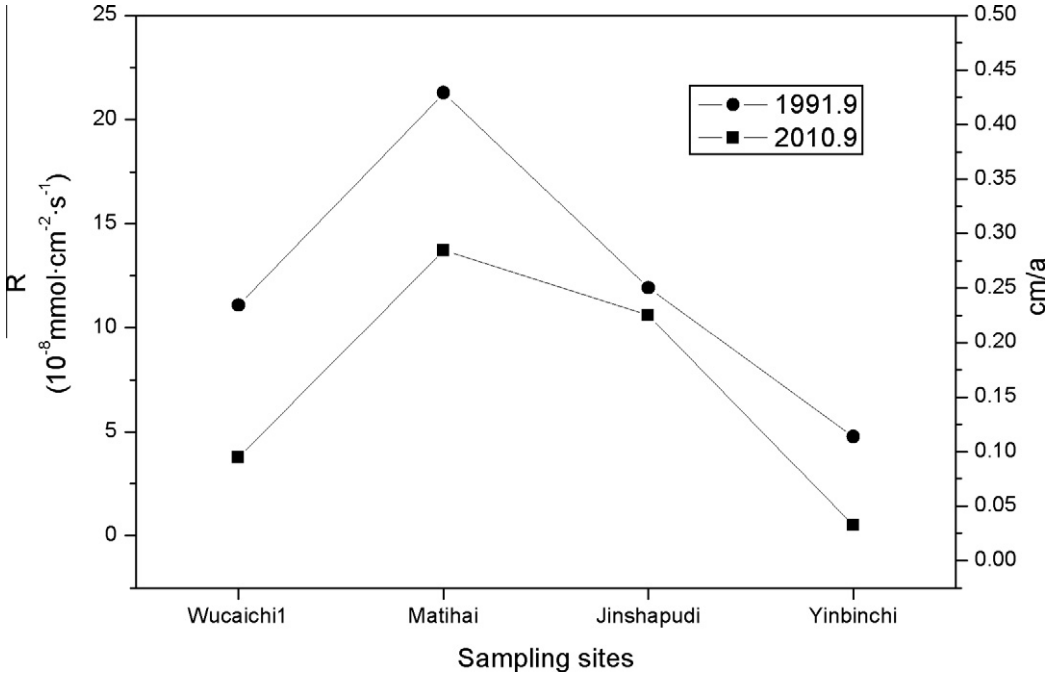

Fig. 7. Comparison of calcite deposition rates between September 1991 and September 2010.

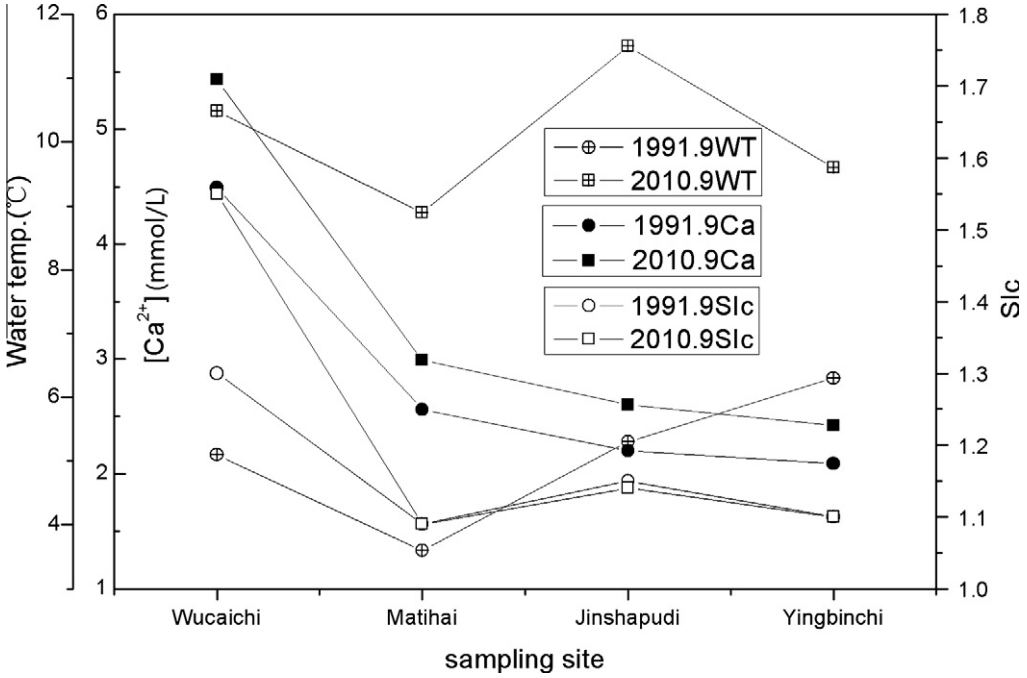

Fig. 8. Comparison of water temperature, Ca^{2+} and SIc between September 1991 and September 2010.

SIc < 0, water is aggressive with regard to calcite and may dissolve it; where SIc = 0, dynamic equilibrium is reached.

3.4. Rainfall

The rainfall was recorded every 15 min with a HOBO rain gauge in Huanglong Ravine with a resolution of 0.2 mm and the data were stored in a HOBO 4-channel data logger. This information is used to understand the climatic control on the water chemistry and the deposition rate of travertine.

3.5. Number of tourists

The daily tourist number was obtained from Huanglong National Scenic Spot Administration for the whole study period, and the relationship between the concentration of PO_4^{3-} in water and the tourist number over the same period was determined.

4. Results and discussion

4.1. Spatial variations in travertine deposition rates

Fig. 6 shows the average travertine deposition rates at the 24 deposition monitoring sites in the four subsystems along flow path in the wet season from May to November.

There is no regular decreasing or increasing trend in the travertine deposition rate along the whole Huanglong Ravine system. In each sub-system as defined in Section 2, the travertine deposition rate generally displayed an increase due to the rising calcite saturation caused by strong continued CO_2 degassing of the spring water entering the stream, and then a decline due to the continued decrease in Ca^{2+} concentration caused by calcite deposition (Wang et al., 2010). Higher travertine deposition rates occur at the sites with higher flow velocity, showing the effect of the diffusion boundary layer determined by flow velocity (Liu et al., 1995; Liu and Dreybrodt, 1997). For example, although Ca concentration and calcite saturation index at sampling site W3 (with slow flow in pool) was even higher than those at sampling site W4 (with fast flow at rimstone dam), W4 has much higher deposition rate than W3 (6.18 times). This clearly demonstrates again the importance of hydrodynamics in controlling travertine deposition (Liu et al., 1995).

4.2. Changes in travertine deposition rate compared to the early 1990s

Liu et al. (1995) examined the travertine deposition rates in the early 1990s. The methods used were very similar. The only difference was that marble tablets were used as substrate. Also

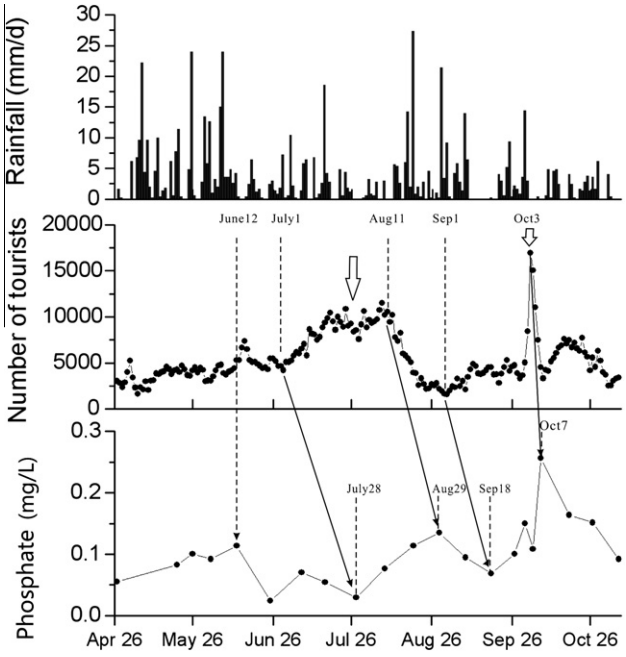

Fig. 9. Temporal variations in concentration of phosphate at sampling site W1 and its relationship with rainfall and tourist numbers in 2010.

the sites used were as closely as possible identical. Fig. 7 shows the comparison with this study. The recent deposition rates show a clear decrease compared with those of 1991 everywhere along the flow path, from 17.8% to 89.5%, with sites W1 (i.e., site No. 8, Liu et al., 1995) and Y (i.e., site No. 1, Liu et al., 1995) showing the largest decrease (65.9% and 89.5%, respectively). In contrast, recent water temperature, Ca^{2+} concentration and SIc are higher than those in 1991 (Fig. 8), which should facilitate carbonate deposition. This gives strong evidence that the decrease in deposition rates is due to the inhibition of calcite deposition by other processes. According to previous studies (Reddy, 1977; Mucci, 1986; Giannimaras and Koutsoukos, 1987; House, 1987; Dove and Hochella, 1993; Bono et al., 2001; Lin and Singer, 2006), this inhibition is very likely caused by PO_4^{3-}, which was introduced into scenic spots by tourism activities.

4.3. Impact of tourism activities on the concentrations of phosphate at Huanglong

Phosphate concentrations in surface water linked to tourism activities in the area is mainly due to pollution from toilet leakage, rubbish flushing by rainfall, and kitchen leakage. All three kinds of wastes are possible sources of PO_4^{3-}. The greater the number of tourists, the more likely is PO_4^{3-} pollution. In order to support this suspicion the temporal variations of the PO_4^{3-} concentration were examined in the stream water in relation to tourism activities,

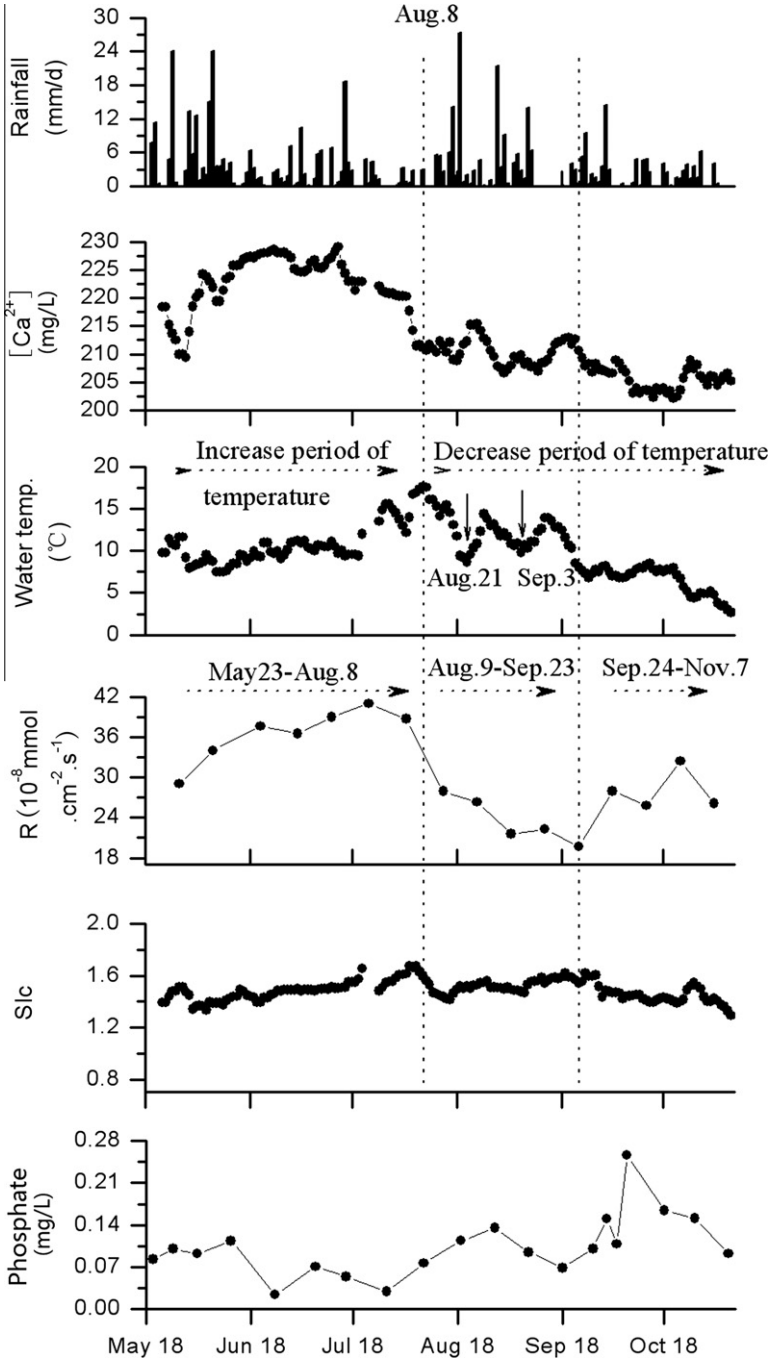

Fig. 10. Temporal variations in travertine deposition rate on the plexiglass substrate at sampling site W4 and its relationship with water temperature, rainfall, phosphate, Ca^{2+} and SIc.

indicated by tourist numbers. It should be noted that at a pH of about eight inorganic PO_4^{3-} is present as $H_2PO_4^-$ and HPO_4^{2-}. For simplicity the term phosphate is used in the following text.

To simplify the explanation, we use the upstream sampling site W1 (close to the tourist trail) as an example of the relationship between the phosphate concentration and tourist numbers. Fig. 9 shows that the phosphate concentrations have significant positive correlation with tourist numbers. For example, there are two peaks in tourist numbers in the experimental period (two large arrows in Fig. 9), and the phosphate concentration shows two peaks as well. This indicates that the phosphate concentration in the stream water has been influenced by tourism activities.

As shown in Fig. 9, the phosphate concentration peaks lag behind tourist numbers some times depending on strong rainfall events. If there were no strong rainfall events, the general lag-time was about 17–27 days. For example, the phosphate concentration kept rising between July 28 and August 29, and then declined, while tourist number rose on July 1 and declined on August 11. Therefore, the lag-time was 27 days and 18 days, respectively. However, if strong rainfall events occurred, there was almost no

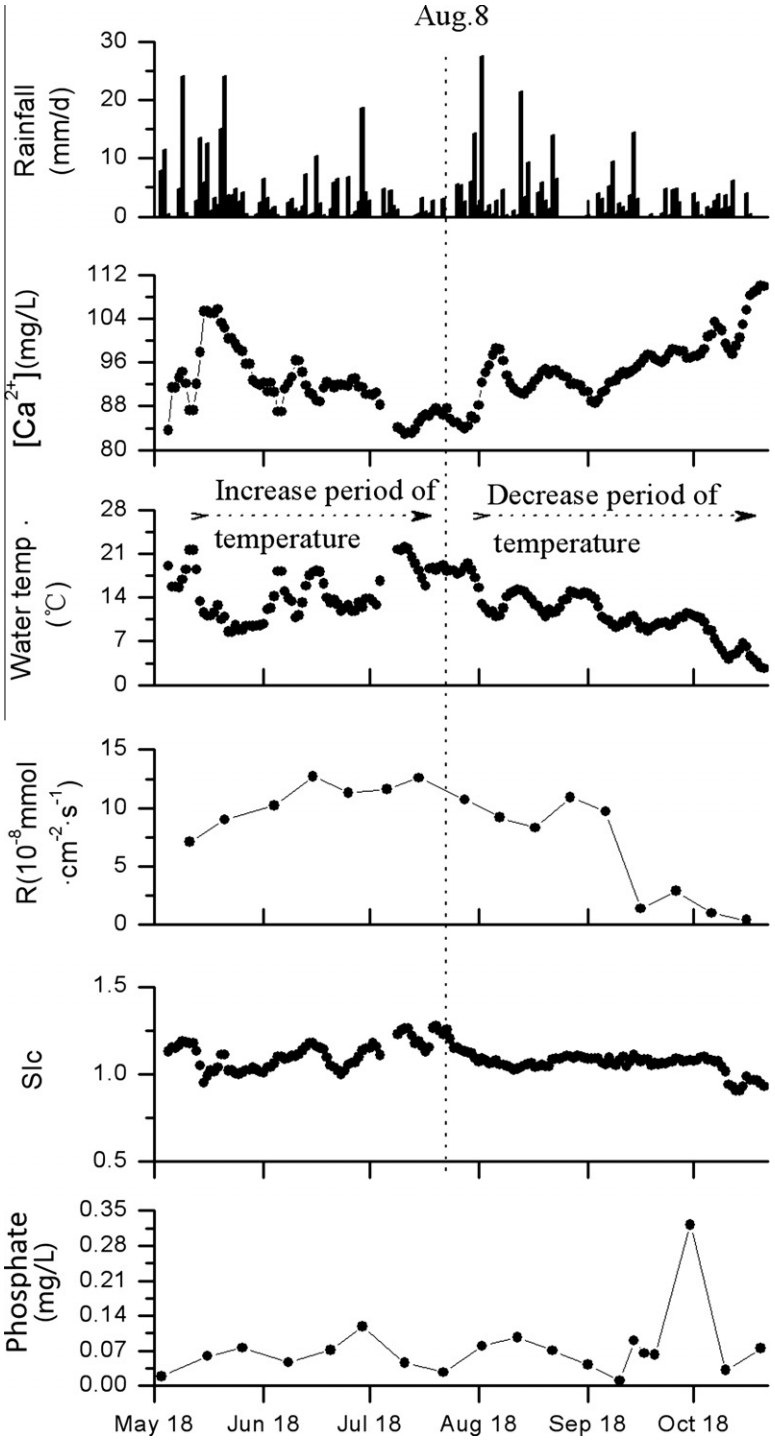

Fig. 11. Temporal variations in travertine deposition rate on the plexiglass substrate at sampling site J8 and its relationship with water temperature, rainfall, phosphate, Ca^{2+} and Slc.

lag-time between phosphate peak and tourist number peak, as shown in Fig. 9 on June 12 and October 3–7. This is due to the flushing effect of rainwater on the wastes from toilets, dustbins and the restaurant in the area. Therefore, it is concluded that tourism activities significantly influence the phosphate concentration in stream water at Huanglong.

4.4. Controls of temporal variations in carbonate deposition rates

According to the theory of the kinetics of karst processes proposed by Dreybrodt (1988), calcite deposition rates in pure carbonate water are determined mainly by calcite saturation index, Ca concentration, temperature, and hydrodynamic conditions. Due to the difference in environmental variables at different sampling sites and times carbonate deposition rates may vary. In the following, the effects of water temperature, dilution effect and inhibition by phosphate are examined jointly.

For an aqueous solution H_2O–CO_2–$CaCO_3$ supersaturated with respect to calcite the deposition rates of calcite (R) are:

$$R = \alpha \cdot (C - C_{eq})$$

where α (cm/s) is a temperature dependent rate constant. The value of α rises linearly from 0.75×10^{-6} at 5 °C to 1.75×10^{-6} at 15 °C (Baker et al., 1998). C is the actual Ca-concentration and C_{eq} is the

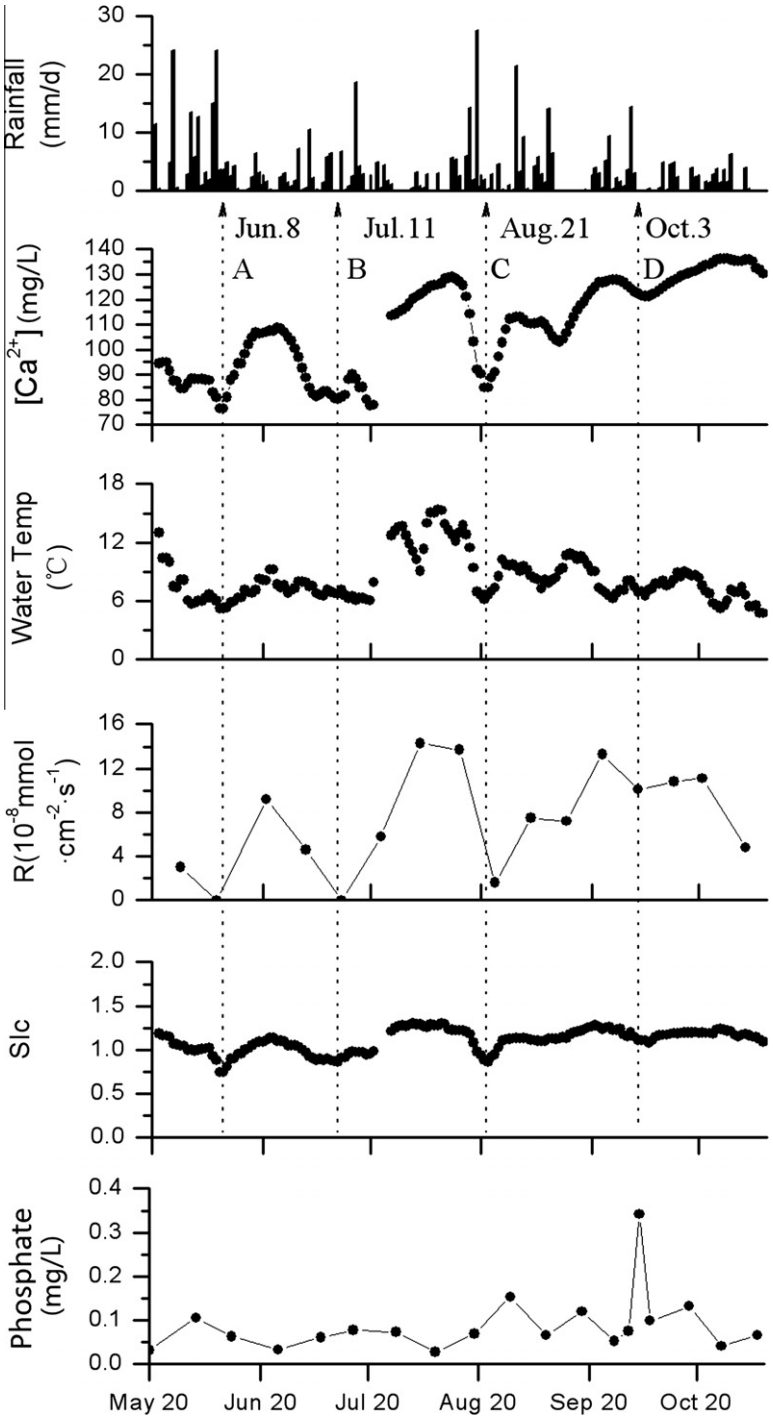

Fig. 12. Temporal variations in travertine deposition rate on the plexiglass substrate at sampling site M4 and its relationship with rainfall, water temperature, phosphate, Ca^{2+} and Slc.

equilibrium Ca-concentration with respect to calcite and the pCO_2 in the water. In Huanglong ravine pCO_2 is approximately 100 Pa and C_{eq} is about 1 mmol/L = 40 mg/L.

4.4.1. Temperature control of temporal variation in calcite deposition rate

Fig. 10 shows the travertine deposition rate (R), the coeval rainfall, water temperature, [Ca^{2+}], SIc, and phosphate at sampling site W4 between May 20 and November 7. Note that this upstream site exhibits extremely high deposition rates, which are not likely inhibited by phosphates. In this case travertine deposition is controlled mainly by water temperature. For example, in the period of increasing temperature from May 23 to August 8, the travertine deposition rate gradually increased with a maximum value of 4×10^{-7} mmol/(cm^2 s) at 15 °C. In the period of decreasing temperature from August 9 to November 7, the travertine deposition rate showed a decreasing trend as well with 2.5×10^{-7} mmol/(cm^2 s) at about 10 °C water temperature. This is in satisfactory agreement with the temperature dependence of α. However, it was also noted that the travertine deposition rate declined to the lowest value during the experimental period from August 12 to September 23 due to the combined effect of dilution and steep temperature decrease caused by the strong rainfall events from August 12 to September 9 (Fig. 10).

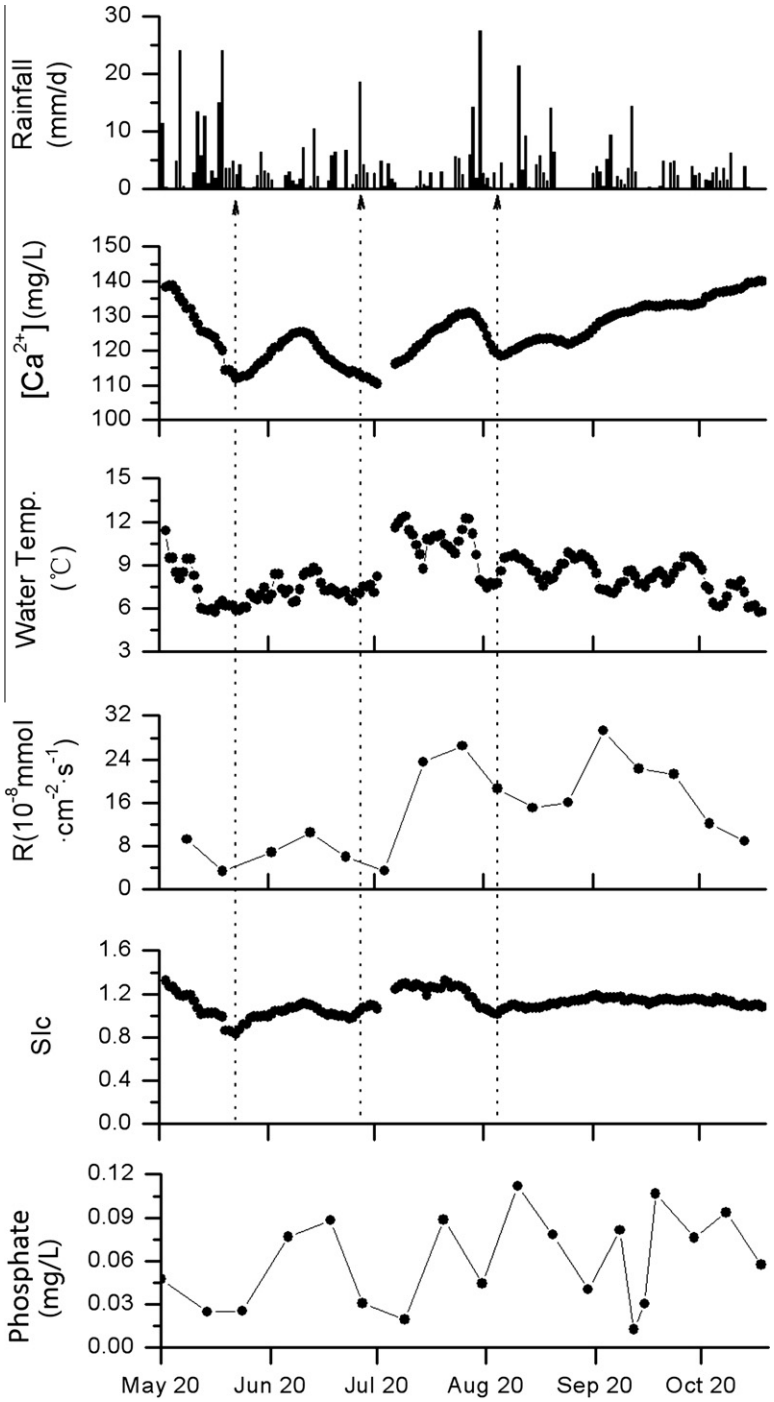

Fig. 13. Temporal variations in travertine deposition rate on the plexiglass substrate at sampling site Z3 and its relationship with rainfall, water temperature, phosphate, Ca^{2+} and SIc.

A similar behavior is observed at sampling site J8 (Fig. 11). At both sites the concentration of PO_4^{3-} is below 1 μmol/L and inhibition is low. Therefore, it is concluded that water temperature is the leading control of travertine deposition at sampling sites W4 and J8. This deposition mechanism is termed water temperature control type.

4.4.2. Dilution control of temporal variation in calcite deposition rate

Fig. 12 shows the travertine deposition rate, the coeval rainfall, water temperature, $[Ca^{2+}]$, SIc and PO_4^{3-} at sampling site M4 (with the snow-melt surface water input) between May 20 and November 7. As can be seen from Fig. 12, there is significant negative correlation between travertine deposition rate and rainfall at sampling site M4, indicating the effect of rainfall dilution on travertine deposition at this site. This is illustrated by a large decrease of $[Ca^{2+}]$ and SIc after rainfall events, especially on June 8, July 11, August 21 and October 3 (A–D in Fig. 12). Note that due to the low concentrations of Ca (<140 mg/L) in contrast to station W4 (>200 mg/L, Fig. 10) the variation of Ca-concentration and SIc exert a significant influence to the rates. It is important to note that for SIc < 0.9 at June 8, July 11, and August 21 deposition stops. This is a well known effect, because a SIc of about 1 is required to drive deposition (Usdowski, 1982). A similar case occurred at the sampling site Z3 with snow-melt surface water input.

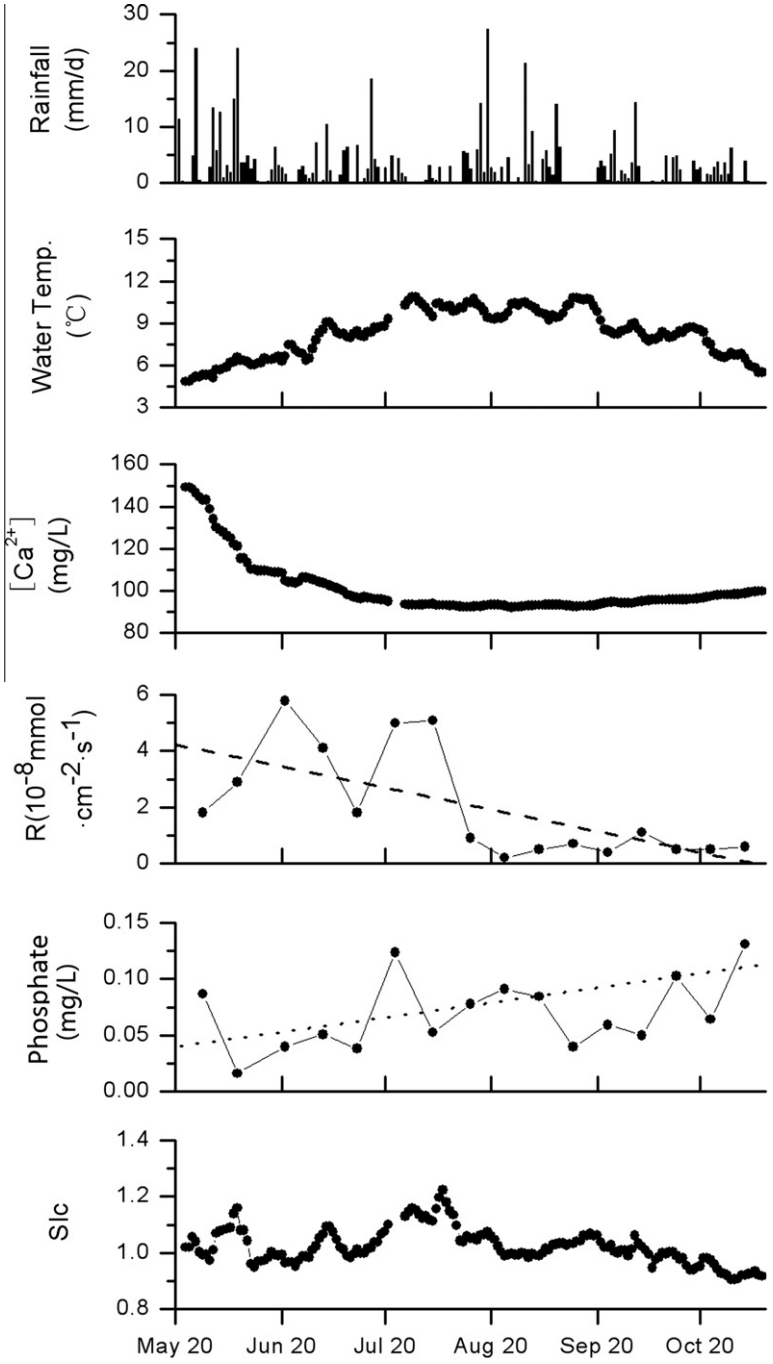

Fig. 14. Temporal variations in travertine deposition rates on the plexiglass substrate at sampling site Y and its relationship with phosphate rainfall, water temperature, Ca^{2+} and SIc. Dashed line and dotted line are trend lines of calcite deposition rates and phosphate concentrations, respectively. During the whole experimental period, calcite deposition rates showed a decreasing trend and phosphate concentrations were opposite.

However, here the temperature amplifies the effect of dilution (Fig. 13).

Therefore, it is concluded that rainfall plus snow-melt water dilution can be a dominating control of travertine deposition at sampling sites M4 and Z3. This deposition mechanism is termed dilution-leading control type.

4.4.3. Phosphate controls of temporal variations in calcite deposition rates

Fig. 14 shows the calcite deposition rate change trend and its relationship with coeval rainfall, water temperature, $[Ca^{2+}]$, SIc and PO_4^{3-} at sampling site Y. During August 20 and September 20 the water temperatures are high and the Ca-concentration is low, but constant. Also SIc is constant above 1. Therefore, one would expect an increase in deposition rates. The opposite, however, is the case. The deposition rates drop to very low values ($<1 \times 10^{-8}$ mmol cm^{-2} s^{-1}), although under similar conditions they were higher by an order of magnitude during July. The only parameter changing during these time spans is the concentration of PO_4^{3-}, which increases with time (Fig. 14). This indicates that the travertine deposition may be inhibited by PO_4^{3-} in the water. Also a weak negative correlation between calcite deposition rate and PO_4^{3-}

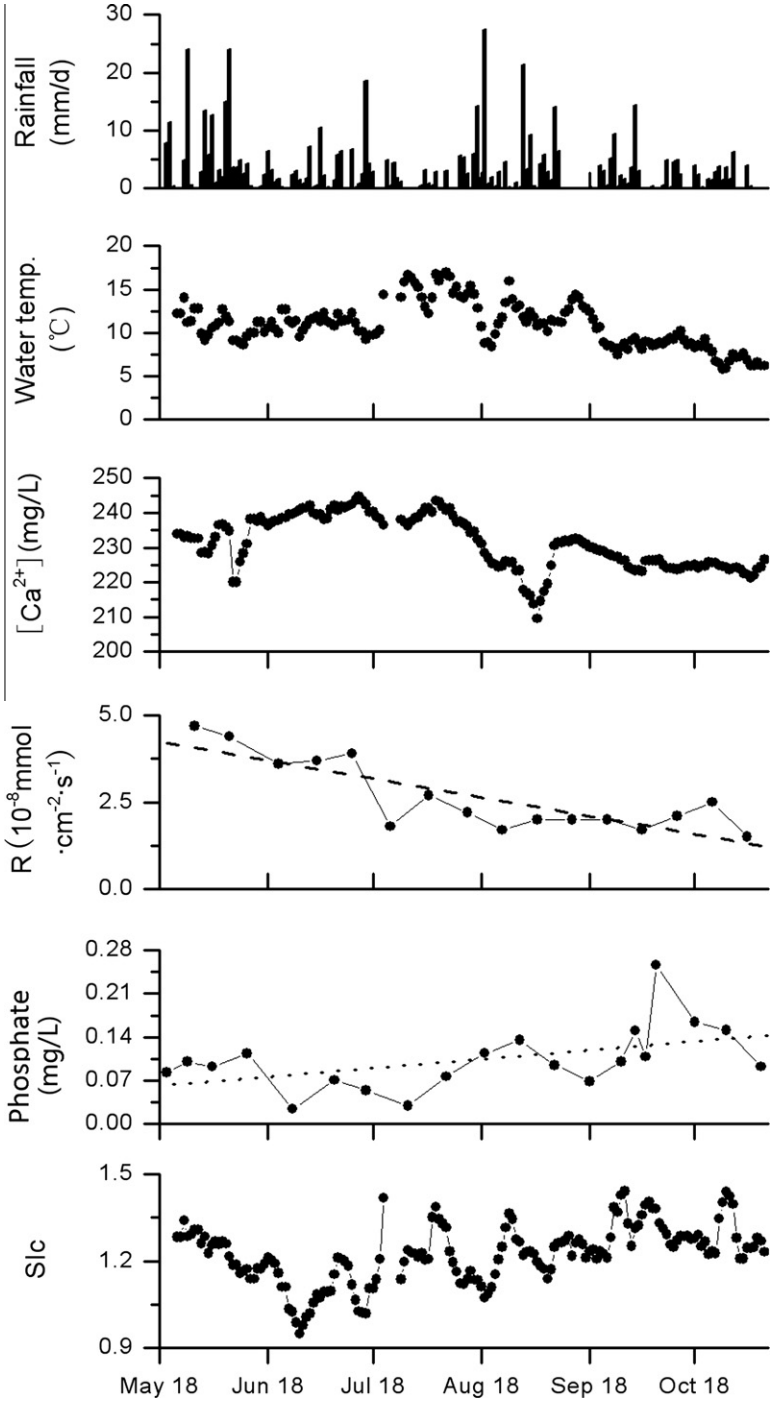

Fig. 15. Temporal variations in travertine deposition rate on the plexiglass substrate at sampling site W1 and its relationship with phosphate, rainfall, water temperature, Ca^{2+} and SIc. Dashed line and dotted line are change trend lines of calcite deposition rates and phosphate concentration, respectively. During the whole experimental period, the calcite deposition rates showed a decreasing trend and phosphate concentration was opposite.

concentration can be seen. Bono et al. (2001) have shown experimentally in a precipitation state test in the field that PO_4^{3-} concentrations as low as 0.1 mg/L cause inhibition of calcite precipitation, which is enhanced at higher concentrations. This is in accordance with the present observations.

Fig. 15 also gives a similar indication at the sampling site W1. During August to October SIc is high, above 1.25, whereas from May to August SIc is lower. Nevertheless the rates are higher (>3.7 mmol cm^{-2} s^{-1}) under those unfavorable conditions than during the more favorable conditions in August to October (<2.5 mmol cm^{-2} s^{-1}). During this later time concentrations of PO_4^{3-} have increased to a high level (>0.14 mg/L). This is a further indication of inhibition. Therefore, it is concluded that inhibition of calcite precipitation by PO_4^{3-} may control the travertine deposition at the sampling sites Y and W1.

5. Conclusions and suggestions for landscape protection

It has been shown that the travertine deposition rate at Huanglong has decreased significantly compared to rates in the early 90s with the largest decrease of 65.9% and 89.5%, respectively, at the sampling sites W1 and Y. It is concluded that the decrease in deposition rate may result from the inhibition of calcite precipitation by PO_4^{3-} pollution caused by tourism activities. In addition, important control patterns of travertine deposition were distinguished along the Ravine. These are water-temperature control and dilution-control.

Therefore, to warrant sustainable use of the travertine landscape, environmental assessment of tourism activities in Huanglong Ravine needs to be performed as early as possible to determine the tourist capacity; meanwhile, more attention should be paid to the management of wastes produced by tourism activities, so as to prevent their harmful impact on the water quality and travertine deposition in the ravine. This applies not only for the travertine of Huanglong, but also for many travertine landscapes worldwide. This work intended to raise attention to this problem and to motivate monitoring of phosphates in such streams.

Acknowledgements

This work was supported by the Hundred Talents Program of the Chinese Academy of Sciences (2006-067), and the National Natural Science Foundation of China (Grant Nos. 40872168 and 41172232). We thank Johannes Birkenstock, Geowissenschaften (FB5), University of Bremen, for performing the XRD and Karl-Heinz Baumann, Geowissenschaften (FB5), University of Bremen, for providing the SEM pictures. We also thank the two anonymous reviewers and the editors for their valuable comments and suggestions, which greatly improved the original manuscript.

References

Baker, A., Genty, D., Dreybrodt, W., Barnes, W.L., Mockler, N.J., Grapes, J., 1998. Testing theoretically predicted stalagmite growth rate with recent annually laminated samples implications for past stalagmite deposition. Geochim. Cosmochim. Acta 62, 393–404.

Bono, P., Dreybrodt, W., Ercole, S., Percopo, C., Vosbeck, K., 2001. Inorganic calcite precipitation in Tartare karstic spring (Lazio, central Italy): field measurements and theoretical prediction on depositional rates. Environ. Geol. 41, 305–313.

Dove, P.M., Hochella, M.F., 1993. Calcite precipitation mechanisms and inhibition by orthophosphate: in situ observations by Scanning Force Microscopy. Geochim. Cosmochim. Acta 57, 705–714.

Dreybrodt, W., 1988. Processes in Karst Systems, Springer Series in Physical Environment. Springer, Heidelberg.

Giannimaras, E.K., Koutsoukos, P.G., 1987. The crystallization of calcite in the presence of orthophosphate. J. Colloid Interface Sci. 116, 423–430.

House, W.A., 1987. Inhibition of calcite crystal growth by inorganic phosphate. J. Colloid Interface Sci. 119, 505–511.

Krawczyk, W.E., Ford, D.C., 2006. Correlating specific conductivity with total hardness in limestone and dolomite karst waters. Earth Surf. Process. Landforms 31, 221–234.

Lin, Y.P., Singer, P.C., 2006. Inhibition of calcite precipitation by orthophosphate: speciation and thermodynamic considerations. Geochim. Cosmochim. Acta 70, 2530–2539.

Liu, Z., Dreybrodt, W., 1997. Dissolution kinetics of calcium carbonate minerals in H_2O–CO_2 solutions in turbulent flow: the role of the diffusion boundary layer and the slow reaction $H_2O + CO_2 \Rightarrow H^+ + HCO_3^-$. Geochim. Cosmochim. Acta 61, 2879–2889.

Liu, Z., Groves, C., Yuan, D., Meiman, J., Jiang, G., He, S., 2004. Hydrochemical variations during flood pulses in the southwest China peak cluster karst: Impacts of $CaCO_3$–H_2O–CO_2 interactions. Hydrol. Process. 18, 2423–2437.

Liu, Z., Li, Q., Sun, H., Liao, C., Li, H., Wang, J., Wu, K., 2006. Diurnal variations of hydrochemistry in a travertine-depositing stream at Baishuitai, Yunnan, SW China. Aquat. Geochem. 12, 103–121.

Liu, Z., Sun, H., Lu, B., Liu, X., Ye, W., Zeng, C., 2010. Wet-dry seasonal variations of hydrochemistry and carbonate precipitation rates in a travertine-depositing canal at Baishuitai, Yunnan, SW China: implications for the formation of biannual laminae in travertine and for climatic reconstruction. Chem. Geol. 273, 258–266.

Liu, Z., Svensson, U., Dreybrodt, W., Yuan, D., Buhmann, D., 1995. Hydrodynamic control of inorganic calcite precipitation in Huanglong Ravine, China: field measures and theoretical prediction of deposition rates. Geochim. Cosmochim. Acta 59, 3087–3097.

Liu, Z., Tian, Y., An, D., Wang, H., Tang, S., Zhang, J., Sun, H., Liu, Y., Zhang, Q., 2009. Formation and evolution of the travertine landscape at Huanglong, Sichuan, one of the World Natural Heritages. Acta Geosci. Sinica 30, 841–847 (in Chinese with English abstract).

Lu, G., Li, X., 1992. A study on cold-water travertine surface depositional landforms in Huanglong scenic spot, Sichuan Province. J. Chengdu Coll. Geol. 19, 55–64 (in Chinese with English abstract).

Lu, G., Zheng, C., Donahoe, R.J., Berry, L.W., 2000. Controlling processes in a $CaCO_3$ precipitating stream in Huanglong Natural Scenic District, Sichuan, China. J. Hydrol. 230, 34–54.

Michaelis, I., Usdowski, E., Menschel, G., 1984. Kinetische Faktoren des $CaCO_3$ Abscheidung und Fraktionierung von C and C. Z. Wasser Abwasser Forsch. 17, 31–36.

Mucci, A., 1986. Growth kinetics and composition of magnesian calcite overgrowths precipitated from seawater—quantitative influence of ortho-phosphate ions. Geochim. Cosmochim. Acta 50, 2255–2265.

Plant, L.J., House, W.A., 2002. Precipitation of calcite in the presence of inorganic phosphate. Colloids Surf. 203, 143–153.

Ralph, G.J., Kevin, R., Brian, W., William, D.D., 1996. Effect of phosphonate inhibitors on calcite nucleation kinetics as a function of temperature using light scattering in an autoclave. Chem. Geol. 132, 215–225.

Reddy, M.M., 1977. Crystallization of calcium carbonate in the presence of trace concentrations of phosphorous-containing anions: I. Inhibition by phosphate and glycerophosphate ions at pH 8.8 and 25 °C. J. Cryst. Growth 41, 287–295.

Reddy, M.M., Nancollas, G.H., 1973. Calcite crystal growth inhibition by phosphonates. Desalination 12, 61–73.

Usdowski, E., 1982. Reactions and equilibria in the systems CO_2–H_2O and $CaCO_3$–CO_2–H_2O – a review. Neues Jahrb. Mineral. Abh. 144, 148–171.

Wang, H., Liu, Z., Zhang, J., Sun, H., An, D., Fu, R., Wang, X., 2010. Spatial and temporal hydrochemical variation of the spring-fed travertine-deposition stream in the Huanglong Ravine, Sichuan, SW China. Acta Carsol. 39, 247–259.

Wigley, T.M.L., 1977. WATSPEC: a computer program for determining equilibrium speciation of aqueous solutions. Brit. Geomorphol. Res. Group Tech. Bull. 20, 1–46.